Comparison of Air-Water and Oil-Water Multi-Phase Flow Experiments in Glass Bead Packs

D. Wildenschild[1,2], K. A. Culligan[3], and B.S.B. Christensen[2], W.G. Gray[4], M.L. Rivers[5]

[1] Department of Geosciences, Oregon State University, Corvallis, OR 97331; [2] Environment and Resources, Technical University of Denmark, DK-2800 Lyngby; [3] Department of Civil Engineering and Geological Sciences, University of Notre Dame, Notre Dame, IN 46556; [4] Department of Environmental Sciences and Engineering, University of North Carolina, Chapel Hill, NC 27599-7431; [5] Consortium for Advanced Radiation Sources and Department of Geophysical Sciences, University of Chicago

Introduction

Understanding of multiphase flow, transport, and reaction processes in porous media is of great importance to problems of groundwater supply and remediation, agricultural irrigation, and oil and gas recovery. However, lack of information about the microscale geometry and the microscale processes that control large scale processes limits our ability to fully simulate multiphase problems. For instance, the wetting-non-wetting interfacial area has a large degree of influence on the mass transfer between contaminants (non-aqueous phase liquids, NAPLs) and the wetting fluid and therefore it is a controlling factor in dissolution of the NAPL, and therefore for the remediation process. Based on this observation, measurement of microscale quantities such as interfacial areas are necessary complements to traditional macroscale measurements.

Although air-water systems are predominant in natural multiphase flow problems, the flow and interaction of water with NAPLs are problems of continued interest. Modern groundwater contamination incidents often begin with the release of a NAPL into the subsurface. Once in the subsurface, the NAPL resides in the vadose zone or the saturated zone as a trapped residual immiscible phase. Determination of a remediation strategy depends upon appropriate characterization of the contaminated site. Studies of NAPL dissolution in porous media have demonstrated that the measurement of saturation alone is insufficient for describing the rate of NAPL dissolution [e.g. 1, 2, 3, 4]. The wetting-non-wetting interfacial area provides a measure of the expected contact with the flushing solutions. It impacts the rate of transfer of NAPL into a flushing agent and will likely be a primary determinant of NAPL removal efficiency [5].

To further explore NAPL-water interaction in the subsurface, the present study presents LNAPL-water data collected using the synchrotron-based computed microtomography (CMT) technique and compares that data to some of the air-water data presented in Culligan et al.[6].

Methods and Materials

The experiments presented here were conducted at the GeoSoilEnviroCARS (GSECARS) beamline and were performed using the same experimental setup as that used to collect the three-dimensional air-water images described in Culligan et al.[6]. Soda lime glass beads were used as the porous medium for both the air-water (AW) experiments presented in Culligan et al.[6], and the oil-water (OW) experiments presented here. The glass bead column was loose-packed in an acrylic sample tube for the AW experiments, while the beads were sintered for the OW experiments and then placed in the tube. Both soda lime glass beads and acrylic tube were preferentially water wet. In both cases, the porosity was 34% and it was computed from the dry image as the number of pixels out of the total number of pixels occupied by air. The water used to saturate the sample was doped with KI (1:6 KI:H_20 mass ratio) in order to enhance the contrast between the wetting and non-wetting phases. We used an energy of 33.3 keV, a level just above the peak photoelectric absorption energy for iodide, for scanning the sample. The resulting voxel size was 17 µm for both the AW and OW experiments, see Figure 1 for an example.

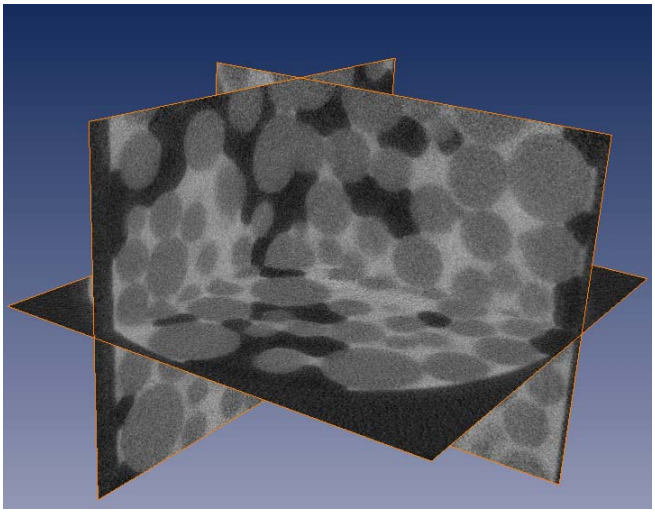

Figure 1: Three-dimensional rendering of an AW data set . White (or light gray) illustrates regions of highest attenuation (wetting-phase), black represents regions of lowest attenuation (non-wetting phase), and gray regions are beads.

Results

Saturation Profiles

Figures 2 and 3 compare the vertical (wetting phase) saturation profiles of both the AW and OW experiments for secondary imbibition and drainage, respectively. As can be seen in the figures, the AW experiments reach much higher wetting phase saturations on imbibition (Figure 2) than the OW experiments, which corresponds to the low residual air phase saturation and relatively high residual oil phase saturation observable in measured capillary pressure-saturation curves. An average residual wetting phase saturation of 5.4% is reached on second AW drainage (Figure 3), while 10.7% is the average value achieved during second OW drainage.

Wetting-Non-Wetting Interfacial Area

The wetting-non-wetting interfacial area, which does not take into account the presence of films, is shown as a function of wetting phase saturation in Figure 4. The macroscopic theory of Hassanizadeh and Gray [7] predicts that, as observed in the present study, the interfacial area will increase from zero as the wetting phase saturation decreases, reach a maximum, and then decrease back to zero as the wetting phase saturation continues to decrease. This model of interfacial area behavior as a function of saturation is supported by numerical modeling studies as well [8, 9, 10]. The maximum interfacial area values in the AW experiments are greater in drainage than in imbibition, which is expected based on consideration of a simple capillary tube. Upon drainage, the interface would be more stretched, whereas upon imbibition it would be flatter [6].

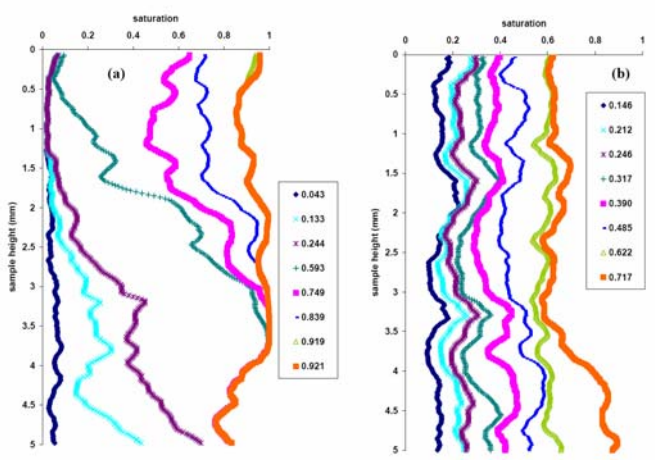

Figure 2. Wetting phase saturation profiles for second imbibition **(a)** air-water **(b)** oil-water. The legends are average wetting phase saturations for the imaged region. Air/oil enters on top, water flows in/out through the bottom.

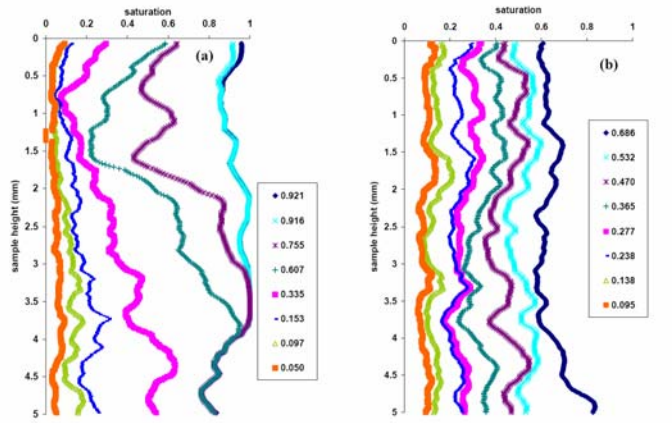

Figure 3. Wetting phase saturation profiles for secondary drainage **(a)** air-water **(b)** oil-water. The legends are average wetting phase saturations for the imaged region. Air/oil enters on top, water flows in/out through the bottom.

As can be seen, the peak OW interfacial areas occur in the 15% to 25% saturation range and are larger than those observed in the AW experiments which occur in the 20% to 35% saturation range. In Figure 5, it can also be seen that in the vicinity of these peak interfacial area values, the oil is located in numerous smaller, more disconnected fluid configurations, while the air is in larger, but fewer and more continuous fluid configurations and that is why we see the peak AW values occurring at a higher saturation than the peak OW values. The reason for the air to be in larger, more continuous fluid configurations, while the oil is in smaller, more disconnected fluid configurations is likely related to differences in the interfacial tension. The interfacial tension between Soltrol 220 and water is 0.0364 N/m, while that between air and water is 0.0681 N/m. The relation between interfacial tension and capillary pressure can be written:

$$p^c = \frac{2\sigma}{r} \qquad (1)$$

where p^c is the capillary pressure, σ is the interfacial tension, and r is the radius of curvature. This means that for a given capillary pressure:

$$r_{ow} < r_{aw} \qquad (2)$$

and therefore the oil will distribute within the water such that its interfacial curvature will be larger than that of the AW interfaces. Such a distribution may be achieved when the oil exists in smaller fluid arrangements.

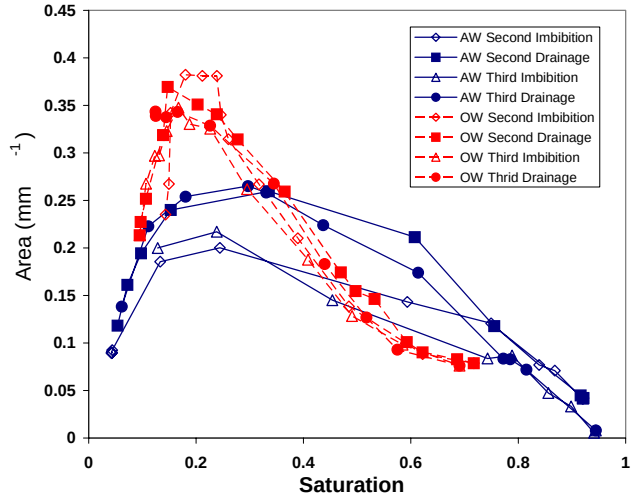

Figure 4: Wetting-non-wetting interfacial area vs. saturation for the air-water (blue) and oil-water (red) experiments. Open symbols are imbibition curves, while closed symbols are drainage curves.

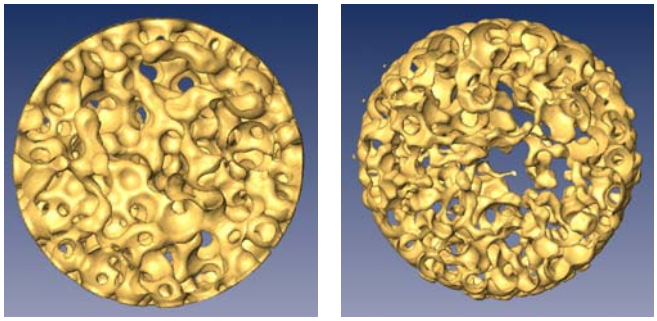

(a) **(b)**

Figure 5: Non wetting phase distributions in three dimensions. **(a)** the air phase is located in larger continuous fluid configurations at s^w=*24.4%* compared to **(b)** the oil phase which is located in smaller and less well-connected configurations at a similar saturation: s^w=*23.9%* , leading to higher interfacial area values at these lower saturations. Both images are from the second imbibition branch.

Discussion and Conclusion

While the dynamics of the air phase have traditionally been neglected in AW experiments, the dynamics of the oil phase cannot be neglected in OW experiments. The air is essentially an inviscid fluid whereas the oil is a viscous fluid flowing in conjunction with the water. This could explain some of the differences observed between the AW and OW experiments. In our capillary-pressure measurements, we assume that the air phase pressure is everywhere at equilibrium with the atmosphere. The more uniform saturation profiles along with the images illustrate that the oil phase connectivity is achieved much sooner than the air phase connectivity in the drainage and imbibition processes. The higher observed residual oil saturation can be seen in the saturation profiles as well as the capillary pressure-saturation curves. From the images, we can see that the residual oil in the OW experiments is arranged in smaller fluid configurations compared to the larger fluid configurations of residual air phase in the AW experiments, likely due to the difference in interfacial tensions between the fluid pairs for the two systems, as discussed previously. These distributions of oil and air lead to the differences in maximum wetting-non-wetting interfacial area, with the OW experiments showing a much higher interfacial area than the AW experiments.

The differences between the AW and OW experiments could also be attributed to small physical differences in the experimental setups. For instance, the glass beads were loose-packed in the AW experiments, whereas they were sintered in the OW experiments, however the same porosity was obtained in the two experiments. While the sintering was done to attempt a tight fit in the cylinder, we believe that some preferential flow occurred along the walls in the OW experiments and did not in the loose-packed AW experiments. It is difficult to ascertain to what degree this wall effect is responsible for some of the observed differences, yet we believe that when limiting our analyses to the cropped center section and to macroscopic variables (saturation, interfacial area, and wetted fraction of the solid surface), this effect can generally be overcome. As mentioned earlier, when a continuous oil connection is made from top to bottom of the sample in the OW experiments, the water phase pressure continues to decrease and thereby drain water from the sample despite the oil presence at the walls.

Microscale experiments such as those presented here have useful macroscale results. For example, mass transfer processes such as NAPL dissolution are typically modeled using an effective rate constant that implicitly combines the effect of interfacial area and the reaction rate constant, despite no knowledge of the specific interfacial area in the system [11]. Therefore, while not explicitly accounted for, interfaces are incorporated into mass transfer models. Thus, the specific interfacial area is a particularly important macroscale variable. In fact, incorporation of this parameter into models will be an important step in the development of robust simulators that correctly describe mass, momentum, and energy transfer between phases [6]. With experiments such as those presented here, interfaces can be accounted for in a variety of models. We have shown that the wetting-non-wetting interface is an important variable, as hypothesized in Gray et al. [12]. These results may also be used as input to numerical simulators or, alternatively, as verification of numerical simulators. It should be kept in mind that the results presented here are for very specialized glass bead porous media systems. It would be very interesting to continue this work on natural systems and see if the same results hold.

Acknowledgments

We thank the entire GSECARS staff for experimental assistance. This work was supported by a National Science Foundation (NSF) Graduate Research Fellowship, NSF grant DMS-0327896, and a grant from the Danish Technical Research Council. Portions of this work were performed at GeoSoilEnviroCARS (Sector 13), Advanced Photon Source (APS), Argonne National Laboratory. GeoSoilEnviroCARS is supported by the National Science Foundation - Earth Sciences (EAR-0217473), Department of Energy - Geosciences (DE-FG02-94ER14466) and the State of Illinois. Use of the APS was supported by the U.S. Department of Energy, Basic Energy Sciences, Office of Energy Research, under Contract No. W-31-109-Eng-38.

References

[1] Miller, C.T., M.M. Poirier-McNeill, and A.S. Mayer, Dissolution of trapped nonaqueous phase liquids – mass transfer characteristics, *Water Resources Research*, *26*(11), 2783-2796, 1990.

[2] Powers, S.E., L.M. Abriola, W.J. Weber, An experimental investigation of nonaqueous phase liquid dissolution in saturated subsurface systems – steady-state mass transfer rates, *Water Resources Research*, *28*(10), 2691-2705, 1992.

[3] Imhoff, P.T., P.R. Jaffe, and G.F. Pinder, An experimental study of complete dissolution of a nonaqueous phase liquid in saturated porous media, *Water Resources Research*, *30*(2), 307-320, 1994.

[4] Nambi, I.M., and S.E. Powers, NAPL dissolution in heterogeneous systems: an experimental investigation in a simple heterogeneous system, *Journal of Contaminant Hydrology*, *44*(2), 161-184, 2000.

[5] Annable, M.D., J.W. Jawitz, P.S.C. Rao, D.P. Dai, H. Kim, and A.L. Wood, Field evaluation of interfacial and partitioning tracers for characterization of effective NAPL-water contact areas, *Ground Water*, *36*(3), 495-503, 1998.

[6] Culligan, K.A.C., D. Wildenschild, B.S.B. Christensen, W.G. Gray, M.L. Rivers, A.F.B. Tompson, Interfacial Area Measurements for Unsaturated Flow Through a Porous Medium, *Water Resources Research*, *in print*, 2005.

[7] Hassanizadeh, S.M., and W.G. Gray, Thermodynamic Basis of Capillary Pressure in Porous Media, *Water Resources Research*, *29*(10), 3389-3405, 1993.

[8] Reeves, P.C., and M.A. Celia, A functional relationship between capillary pressure, saturation, and interfacial area as revealed by a pore-scale network model, *Water Resources Research*, *32*(8), 2345-2358, 1996.

[9] Berkowitz, B., and D.P. Hansen, A Numerical Study of the Distribution of Water in Partially Saturated Porous Rock, *Transport in Porous Media*, *45*(2), 303-319, 2001.

[10] Dalla, E., M. Hilpert, and C.T. Miller, Computation of the interfacial area for two-fluid porous medium systems, *Journal of Contaminant Hydrology*, *56*, 25-48, 2002.

[11] Johns, M.L., and L.F. Gladden, Magnetic Resonance Imaging Study of the Dissolution Kinetics of Octanol in Porous Media, *Journal of Colloid and Interface Science*, *210*(2), 261-270, 1999.

[12] Gray, W.G., A.F.B. Tompson, and W.E. Soll, Closure conditions for two-fluid flow in porous media, *Transport in Porous Media*, *47*(1), 29-65, 2002.